CHARACTERIZATION OF ANISOTROPIC THERMAL CONDUCTIVITY FOR BIG AREA ADDITIVE MANUFACTURING WITH POLYMERS

Artem A. Trofimov¹, Hsin Wang¹, Ahmed Arabi Hassen¹, Halil Tekinalp², Vlastimil Kunc², Seokpum Kim², Soydan Ozcan²

ABSTRACT

Additive manufacturing with polymers has been used mainly for prototyping. A recent development of Big Area Additive Manufacturing (BAAM) at Oak Ridge National Laboratory has opened its applications in the mold and die industry. A numerical simulation and prediction for a mold heating performance requires accurate anisotropic thermal properties of the printed material, which are challenging to obtain and often requires the use of multiple techniques. The transient plane source (TPS) technique has been widely used due to its ability to measure the thermal properties of an extensive range of materials (solids, liquids, powder). Despite the capability to characterize thermal conductivity (k) of isotropic and anisotropic materials, the measurements of latter materials are limited to the cases, where the samples have the same thermal conductivity (k)along x- and y-axis that form the radial plane. In this work, the method for a characterization of k in all three dimensions is developed, and the application of TPS is extended to the determination of thermal properties along the x-, y-, and z-axis individually. The materials are represented by additively manufactured polymers including polylactic acid (PLA) and styrene maleic anhydride (SMA). The developed method consists of (1) a determination of the heat capacity of the polymers by means of TPS in combination with the model developed in this work for the data analysis procedure, (2) a machining three types of cylindrical samples from the same material, with the height corresponding either to x-, y-, or z-direction of printing, and (3) a determination of axial thermal conductivity employing anisotropic model and using previously determined heat capacity

Corresponding authors: A. Trofimov¹, trofimovaa@ornl.gov; H. Wang¹, wangh2@ornl.gov

Notice: This manuscript has been authored by UT-Battelle, LLC, under Contract No. DE-AC0500OR22725 with the U.S. Department of Energy. The United States Government retains and the publisher, by accepting the article for publication, acknowledges that the United States Government retains a non-exclusive, paid-up, irrevocable, world-wide license to publish or reproduce the published form of this manuscript, or allow others to do so, for the United States Government purposes. The Department of Energy will provide public access to these results of federally sponsored research in accordance with the DOE Public Access Plan (http://energy.gov/downloads/doe-public-access-plan).

¹ Materials Science & Technology Division, Oak Ridge National Laboratory, Oak Ridge, TN

² Energy and Transportation Science Division, Oak Ridge National Laboratory, Oak Ridge, TN

1. INTRODUCTION

Additive manufacturing (AM) has become a significant part of the industry due to the rapid production of various parts [1, 2] and the accurate control of deposition [3]. The recent development of large-scale printing systems has opened new applications of additive manufacturing in the mold and die industry. For example, using Big Area Additive Manufacturing (BAAM), Oak Ridge National Laboratory (ORNL) has printed a trim tool for Boeing 777X, a hand layup tool for Shelby Cobra hood, a tool for vacuum-assisted resin transfer molding (VARTM), and a mold for a 13-meter long windmill blade [4].

Important part of AM application in the aforementioned industry is a numerical simulation and prediction under service loading for molding or tooling. As seen in Ref. [5], ORNL has developed a computational capability to predict the thermally expanded geometry of an additively manufactured in-autoclave mold and to machine the surface with the updated geometry. The accuracy of this approach highly depends on the measurement of the thermal properties. Obtaining these properties is often challenging since extruded specimen can have anisotropic thermal properties, e.g., due to printing direction or reinforcement with the fibers. As a result, multiple techniques and instruments are frequently needed to measure such properties as thermal conductivity in three different directions (along x-, y-, and z-axis). One choice is to perform the measurements by means of laser flash technique [6] and differential scanning calorimetry (DSC) [7], where the former provides a thermal diffusivity of the material along the single axis parallel to the laser beam, and the latter allows to obtain the specific heat capacity. In such manner, the thermal conductivity is obtained by combining the heat capacity, the directional thermal diffusivity, and the separately measured density.

Alternatively, Transient Plane Source (TPS) technique, commonly referred as the Hot Disk method [8-11], has been one of the popular tools in recent years. TPS allows for the evaluation of thermal properties at a fast rate and using the samples as small as a few millimeters. The method has been used for a wide variety of materials including bulk solids and thin films [9, 12-14], liquids [15, 16] and powders [17]. Additionally, TPS can test both isotropic and anisotropic samples [18, 19]; however, latter requires prior knowledge of material's heat capacity as well as the same thermal conductivity in the radial direction.

In this work, the heat capacity measurements using TPS have been modified to provide more accurate results for the materials with low thermal conductivity. The TPS method has been extended to the evaluation of thermal conductivity along three individual axes on the specimen of additively manufactured polylactic acid (PLA) and styrene maleic anhydride (SMA).

2. EXPERIMENTATION

2.1 Principle of TPS technique: thermal conductivity

Thermal conductivity measurements using TPS commonly consist of the following steps: (1) the sensor, represented by a double spiral made from nickel and sealed between two thin Kapton layers, is sandwiched between two pieces of the same sample to be tested, (2) using an input power defined by the user, a constant current is passed through a sensor, and (3) simultaneously, the change of the sensor's temperature is recorded as a function of time. An experimental setup is illustrated in Figure 1.

The sensor is a resistor/thermometer and acts both as a heater and as a temperature sensor. If the tested samples are isotropic then the temperature increase of the sensor is related to the thermal properties of the surrounding material as [20]:

$$\Delta T(\tau) = P_0(\pi^{3/2} r k)^{-1} D(\tau) \tag{1}$$

where k is the thermal conductivity of the tested material, P_0 is the input power, $\Delta T(\tau)$ is the timedependent temperature increase of the TPS sensor, $\tau = (t/\theta)^{1/2}$, t is the time from the beginning of the transient measurement, $\theta = r^2/\alpha$ is the characteristic time, r is the radius of the sensor, α is the thermal diffusivity of the tested material, and $D(\tau)$ is a dimensionless time function that takes into account the conducting pattern of the disk-shaped sensor consisting of n number of concentric rings of nickel; n depends on the used sensor, and $D(\tau)$ is defined elsewhere [8, 20].

Using θ as an adjustable parameter, experimental data can be linearly fitted to Eq. (1) when $\Delta T(\tau) \sim D(\tau)$, which allows to obtain the thermal diffusivity α of the sample and the value of the slope, $P_0(\pi^{3/2}rk)^{-1}$, which is used to extract a thermal conductivity k.

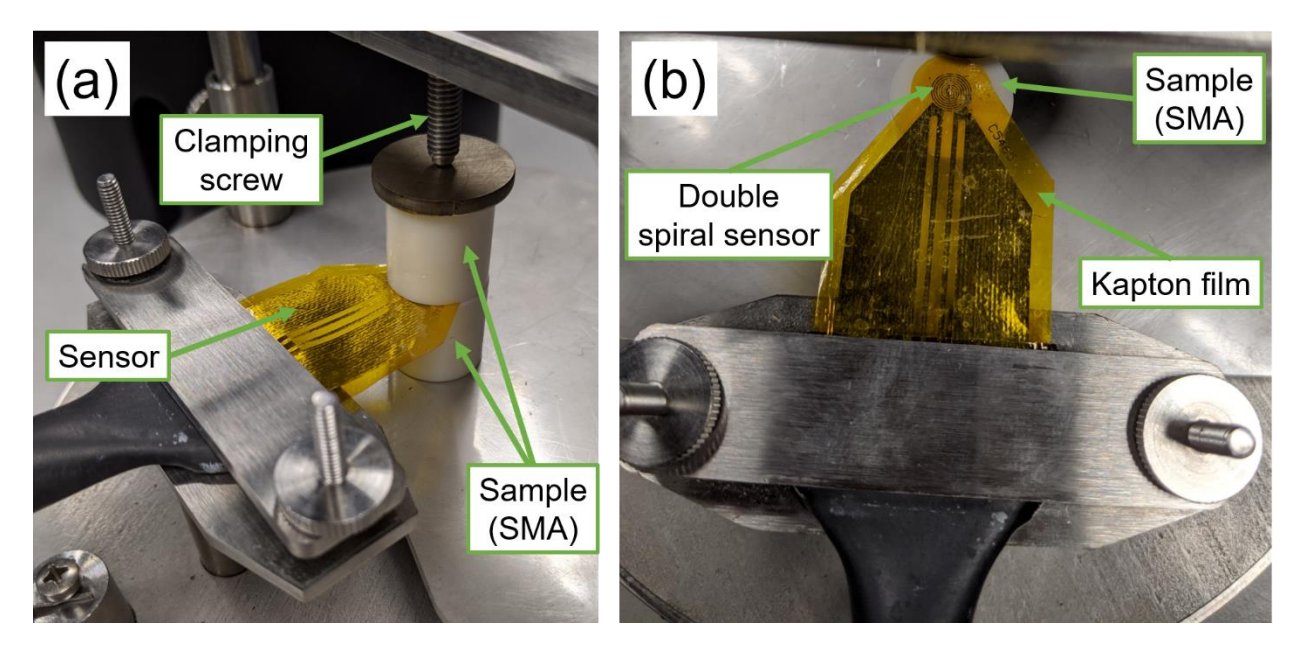


Figure 1. (a) TPS set-up depicting the sensor positioned between two reference samples forming a sample-sensor-sample arrangement. Brass free weight is used to ensure a good contact between the sensor and the samples. (b) Double spiral sensor sealed by Kapton.

In the case of anisotropic material, where the thermal properties are the same along the two axes forming a radial plane (e.g., x- and y-axis) but different from those along the third axis (e.g., z-axis), the performed experiments are the same, but the fitting equation is

$$\Delta T(\tau_x) = P_0[\pi^{3/2} r(k_x k_z)^{1/2}]^{-1} D(\tau_x) , \qquad (2)$$

where $k_x = k_y \neq k_z$, $\tau_x = (t/\theta_x)^{1/2}$, and $\theta_x = r^2/\alpha_x$. Accordingly, θ_x is used as a fitting parameter to calculate thermal diffusivity α_x along the x-axis. Next, the previously determined density, ρ , and

the heat capacity, C_p , are used to calculate $k_x = \alpha_x \rho C_p$, and the axial thermal conductivity, k_z , is obtained from the determined k_x and the slope of the line described in Eq. (2) [18, 19].

The situation of anisotropic material with $k_x \neq k_y \neq k_z$ is subject of this investigation and, therefore, is discussed in the Results section.

2.2 Principle of TPS technique: heat capacity

In the specific heat capacity experiments, a TPS sensor is attached to the bottom side of the high conductivity sample holder with a diameter of 20 mm and a height of 5 mm. Evaluation of the heat capacity consists of at least two measurements: reference measurement in order to acquire transient heating profile of the sample holder, and the sample+reference measurement (sample holder with the tested material placed inside). The method is based on the assumption of constant temperature gradients inside the holder-sample assembly, neglecting the heat losses to the surrounding. Comparative analysis of two transient profiles (reference versus sample+reference) allows evaluation of sample's heat capacity [21]:

$$mC_{\rm p} = P_2/\delta_2 - P_1/\delta_1 \,, \tag{3}$$

where P_1 and P_2 are the input power for the reference and sample+reference measurements, respectively, and $\delta = dT/dt$ is the time derivative of the temperature within the analyzed segment of the transient curve.

2.3 Materials and Methods

Neat polylactic acid (PLA) and styrene maleic anhydride (SMA) were used as the test materials. A part with a hexagon shape was printed for each material. The samples were prepared from the hexagons by cutting and machining. The samples for the thermal conductivity experiments had a cylindrical shape with the dimensions of 20 mm in diameter and 20 mm in height, where the height corresponded either to x-, or y-, or z-directions of the printing. The samples for the heat capacity measurement had a disk shape with the dimensions of 20 mm in diameter and 4 mm in height. Three groups of samples were prepared to repeat the same test three times for a statistical analysis. For each group and each material, six samples were prepared for the conductivity measurement (two samples for each direction) and one sample was prepared for heat capacity measurement (= 7 samples for each test group). Since we are testing three times for two materials, the total number of samples prepared are 42 samples (= $7 \times 3 \times 2$). Figure 2(a-b) shows the shapes and the dimensions of the samples, and Figure 2(c-d) shows the actual appearance of the samples.

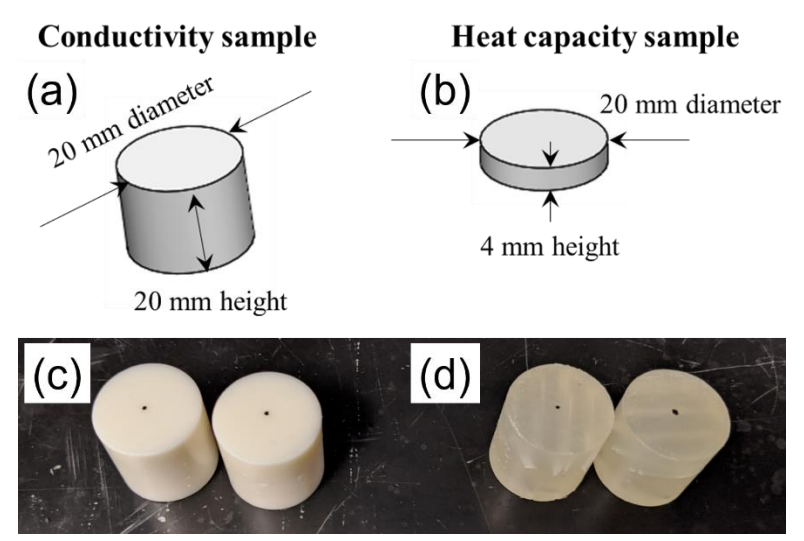


Figure 2: Sample shape and dimensions for (a) thermal conductivity measurement and (b) heat capacity measurement. (c) Styrene maleic anhydride (SMA) and (d) polylactic acid (PLA).

The heat capacity and the thermal conductivity of the investigated materials were measured by a hot disk thermal constant analyzer (Hot Disk Inc., Sweden). A TPS 3500 Hot Disk system with a bridge circuit, a digital voltmeter, and a data analysis module was used.

The heat capacity experiments were sensitive to the change of the surrounding temperature and, in order to maintain constant initial temperature of the holder-sample assembly, it was placed inside the temperature platform (see Figure 3). The input power was 160-410 mW, and the duration of the measurements was 40-160 sec. Two hours of waiting time was allowed between the measurements in order to establish reproducible isothermal conditions at the start of the measurements. The analysis procedure of the data to extract the heat capacity was modified as part of this work, and, therefore, is discussed in Results section. MACOR glass ceramic with the known heat capacity was used as a reference in order to establish the procedure.

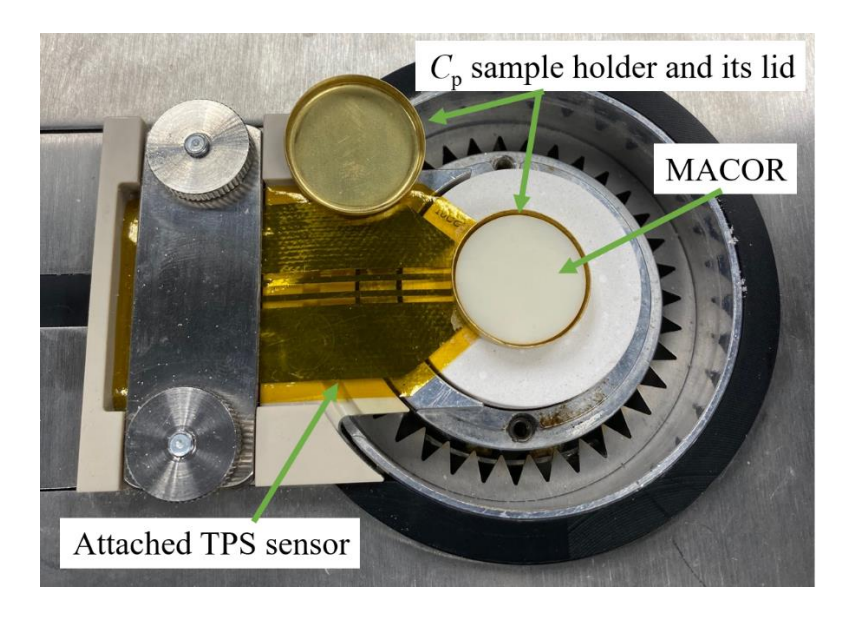


Figure 3. Heat capacity holder-sample (MACOR) assembly with the sensor attached to the bottom of the holder and placed inside the temperature platform. During experiments, the lid is closed, and the assembly is covered with thermal isolation to provide constant initial temperature

The thermal conductivity measurements were performed using anisotropic module and the Hot Disk sensors with the radius of 3.189 mm. The input power was 30-35 mW, and the duration of the measurement was 40-80 sec. Thirty minutes of waiting time was allowed between the measurements in order to establish the reproducible isothermal conditions. The measurements were repeated three times for each set of parameters. The experiments were performed at room temperature and ambient conditions under stainless steel cover to avoid temperature fluctuations from drafts of air to the sample.

3. RESULTS

3.1 Specific heat capacity

Comparative analysis of two transient heating profiles (sample holder alone and holder-sample assembly) allows evaluation of sample's heat capacity. Analysis procedure requires to establish constant temperature gradients inside the holder and sample assembly during the experiment and analyze corresponding portions of the experimental curves. During the experiment, 200 datapoints are recorded regardless the measurement duration, and the standard procedure recommends analyzing last 100 points, as shown in Figure 4a, assuming that the sample has a uniform temperature during this time window. Nevertheless, this assumption is often invalid, especially for low conductive materials, due to slow heat propagation and increasing role of heat loss for long measuring time. As a result, the window of last 100 points does not always correspond to the portion of the transient profile with the constant temperature gradients and can yield erroneous or even negative heat capacity values.

Adl-Zarrabi et al [22] suggested to analyze the data in a variety of windows, where the data point intervals are defined as [A; 2A], [A+2; 2(A+2)], etc., where A is the first selected datapoint (for

example, points [10;20], [12;24], ..., [98-196], [100-200]). The results should give a curve with a maximum value corresponding to the specific heat of the analyzed material (Figure 4b). The presence of aforementioned heat capacity curve can be assigned to the fact that during earlier time windows the calculated heat capacity increases because the sample has not reached a uniform temperature, while at later times the heat loss starts to dominate the measurement and the heat capacity decreases. While, the procedure might give the correct value in some cases, it might also overestimate the heat capacity as shown in Figure 4b on the example of reference MACOR sample.

Therefore, in addition to the aforementioned improvement, the conditions of the analysis need to be modified even further. Besides the analysis of the variety of windows, it should be equal time windows (e.g., every five seconds), and one needs to monitor the temperature increase of both the sample holder, $\Delta T_{\rm ref}$, and the holder-sample assembly, $\Delta T_{\rm sample}$, within the time window of analysis. The portion of the transient profiles, where both assemblies have similar temperature increase (i.e., $\Delta T_{\rm ref} - \Delta T_{\rm sample} \rightarrow 0$) corresponds not only to the time window where their temperature gradients are constant, but also to the window where the gradients are the same, providing accurate heat capacity evaluation (Figure 4c).

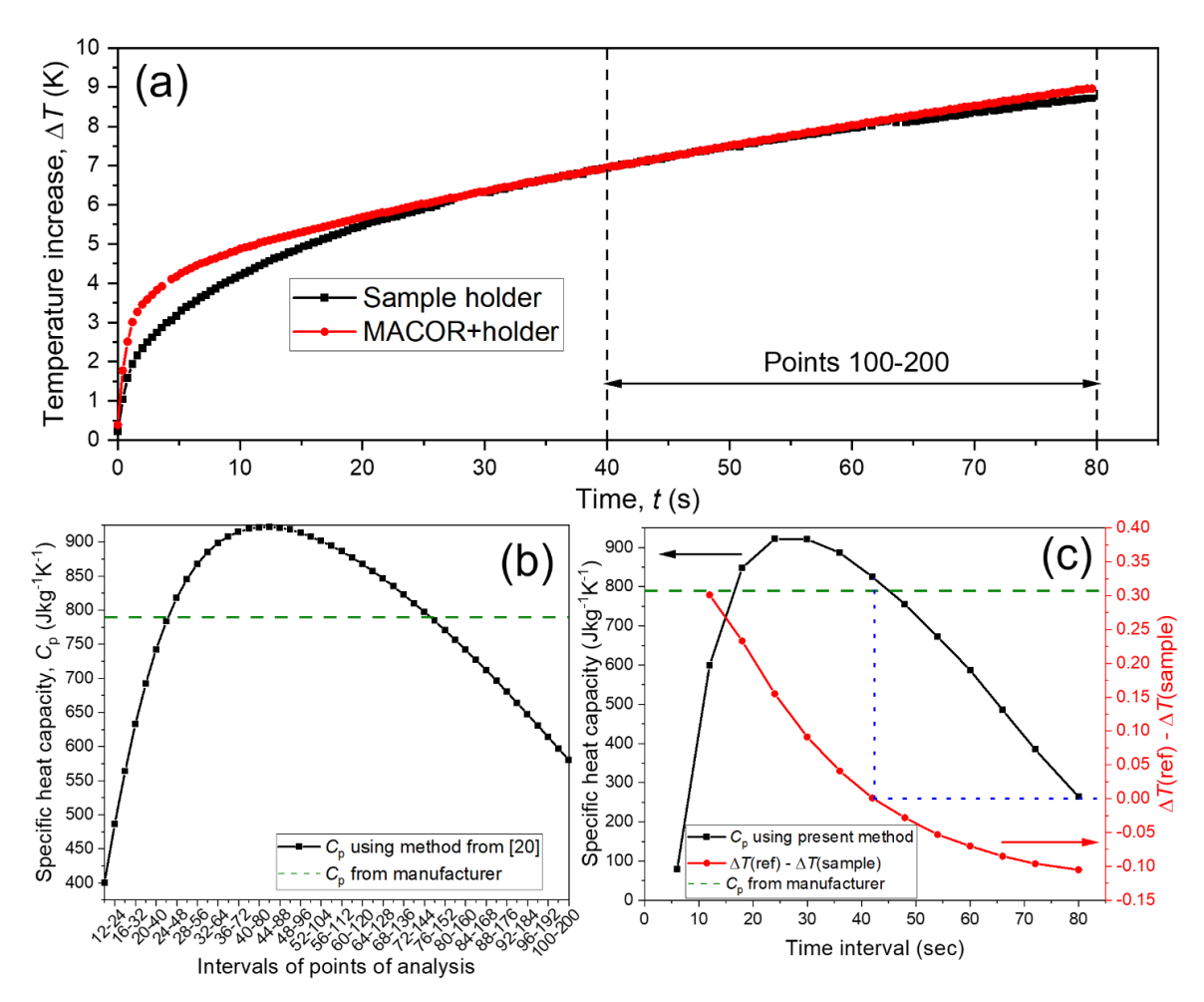


Figure 4. (a) Transient heating profiles of the sample holder and holder-sample (MACOR) assembly during the heat capacity measurements for 80 s using TPS. (b) Specific heat capacity curve obtained using the method from [22]. (c) Specific heat capacity curve obtained using the

method presented in this work, and the corresponding difference between the temperature increase of the sample holder, ΔT_{ref} , and the holder-sample assembly, ΔT_{sample} . Time intervals in (c) were 5 sec each and the *x*-axis values correspond to the end of the given interval.

Using proposed analysis, specific heat capacity of MACOR reference and two additively manufactured polymers (PLA and SMA) were evaluated as shown in Figure 5a. Results for the MACOR showed a good agreement with the reported value by manufacturing company. The specific heat capacity of PLA was within the range of literature values; however, it should be noted that the reports on C_p of PLA have a significant variation from 1300 J/kgK to 1800 J/kgK [23-25]. Specific heat capacity of SMA was not available in the literature to the best of authors' knowledge.

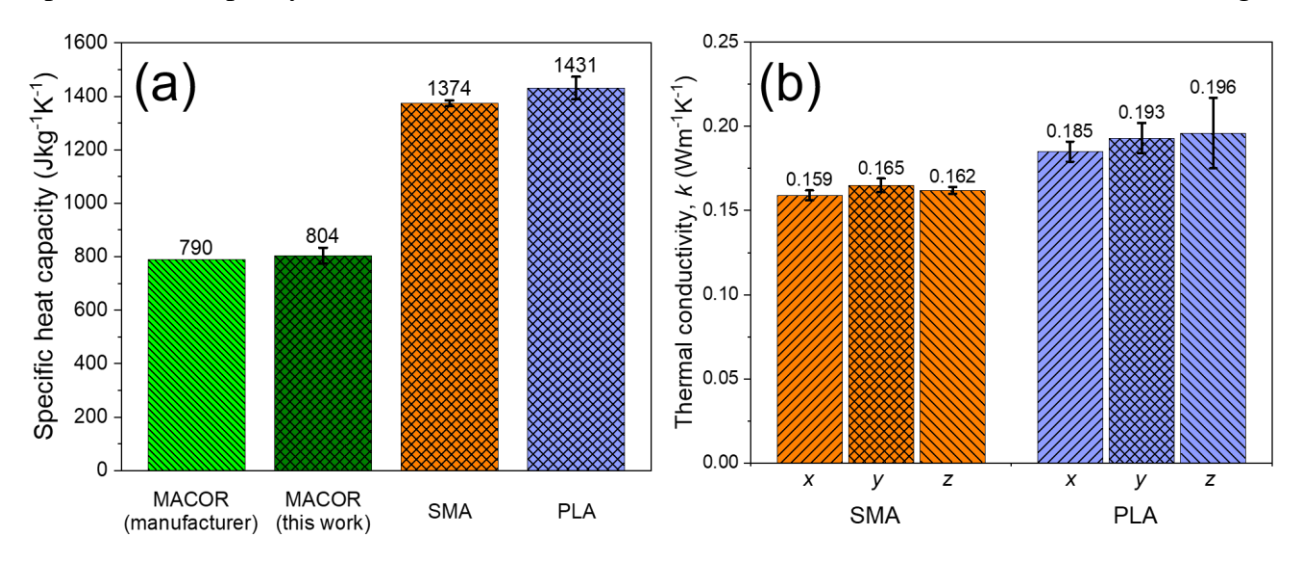


Figure 5. (a) Specific heat capacity of MACOR, SMA, and PLA obtained using the analysis proposed in this work. (b) Thermal conductivity of SMA and PLA for *x*-, *y*-, and *z*-axis.

3.2 Thermal conductivity

Initially, the attempts were made to obtain a thermal conductivity in three distinct directions (x-, y-, and z-axis) using one-dimensional measurements with TPS. Three types of samples of the same material were cut in the shape of cylindrical rod having the direction of the sample's length along x-, y-, or z-axis and the diameter of the samples closely matching the diameter of the used TPS sensor. Similar diameters of the sensor and the samples are necessary to establish a one-dimensional heat propagation in the direction of the rod length, and undisturbed air around the samples is typically adequate to minimize heat flow and heat loss in the radial direction. However, it was found that low thermal conductivity of the investigated polymers required longer than recommended measuring time preventing performance of the measurements without the influence of heat loss.

Consequently, the strategy was changed to the use of the TPS anisotropic model, which normally allows the evaluation of two types of thermal conductivity: radial and axial. In the present case,

the thermal conductivity was assumed to be different in all three directions, which would result in the erroneous values of radial conductivity, but it would still allow the evaluation of axial thermal conductivity, as long as the heat propagation was limited to within the sample. Therefore, three types of samples having axial direction cut along x-, y-, or z-axis were still required. Further steps of the method are similar to the standard TPS method described in Experimentation section, where the heat capacity was measured directly with TPS (Figure 5a). The transient profile was fitted to the anisotropic model in order to calculate the thermal properties of the materials, and only values of axial thermal conductivity, shown in Figure 5b, were used as a final result.

The thermal conductivity of SMA, averaged over three axes, was $k_{\text{SMA}} = 0.163 \pm 0.004$ W/mK, similar to the reported value of 0.170 W/mK [26, 27], and the thermal conductivity of PLA averaged over three axes was $k_{\text{PLA}} = 0.191 \pm 0.014$ W/mK, which was within the reported range of 0.130-0.210 W/mK [23, 26, 28]. Additionally, the thermal conductivities of each polymer were close between three different axes (Figure 5b), indicating that the printing direction did not have a strong influence on the thermal conductivity.

4. SUMMARY AND CONCLUSIONS

This work presented a modified data analysis of the Transient Plane Source (TPS) heat capacity experiments in order to accurately evaluate the heat capacity of the tested materials and established a procedure to obtain the thermal conductivity in three different directions using anisotropic model of the TPS technique. In order to accurately evaluate the C_p value, the standard heat capacity experiment should follow by the analysis of the variety of equal time windows with simultaneous monitoring of the temperature increase of both the sample holder, $\Delta T_{\rm ref}$, and the holder-sample assembly, ΔT_{sample} , within the time window of analysis. It was shown on the example of a commercial MACOR glass-ceramic that the time window where $[\Delta T_{\text{ref}} - \Delta T_{\text{sample}} \rightarrow 0]$ should yield an accurate heat capacity value. The heat capacity of additively manufacture polylactic acid (PLA) and styrene maleic anhydride (SMA) was also evaluated and used for the thermal conductivity measurements. The developed method to extract the thermal conductivity in three different directions included (1) a determination of the heat capacity as described above, (2) a machining of three types of cylindrical samples from the same material, with the height corresponding either to x-, or y-, or z-direction of printing, and (3) a determination of the axial thermal conductivity using anisotropic model. The results were in an agreement with the literature and showed that the printing direction did not have a strong influence on the thermal conductivity of SMA and PLA.

Acknowledgment

This research is sponsored by the US Department of Energy (DOE), Office of Energy Efficiency and Renewable Energy, Advanced Manufacturing Office, under contract DE-AC05-00OR22725 with UT-Battelle LLC. For large-scale additive manufacturing, the printing equipment was provided by Cincinnati Incorporated, a manufacturer of metal and additive manufacturing equipment, headquartered in Harrison, Ohio (www.e-ci.com). The printing material for large-scale additive manufacturing was provided by Techmer PM, a material design and manufacture company headquartered in Clinton, TN.

References

- [1] S.H. Ahn, M. Montero, D. Odell, S. Roundy, K. Wright Paul, Anisotropic material properties of fused deposition modeling ABS, Rapid Prototyping Journal, 8 (2002) 248-257.
- [2] V. Kunc, A.A. Hassen, J. Lindahl, S. Kim, B. Post, L. Love, Large scale additively manufactured tooling for composites, 15th Japan International SAMPE Symposium and Exhibition, Tokyo, Japan, 2017.
- [3] J. Scott, N. Gupta, C. Wember, S. Newsom, T. Wohlers, T. Caffrey, Additive Manufacturing: Status and Opportunities, Washington DC, 2012, pp. 1-29.
- [4] B. Post, P. Chesser, A. Roschli, L. Love, K. Gaul, Large-Scale Additive Manufacturing for Low Cost Small-Scale Wind Turbine Manufacturing, Oak Ridge National Laboratory, Oak Ridge, TN, 2018.
- [5] A. Hassen, A. Lambert, J. Lindahl, D. Hoskins, C. Duty, S. Simunovic, C. Chin, V. Oancea, L. Love, V. Kunc, S. Kim, Simulation Assisted Design for an Additively Manufactured Autoclave Tool Accounting for an Anisotropic Expansion, in: The Composites and Advanced Materials Expo (CAMX 2019), Anaheim, CA, 2019.
- [6] ASTM E1461-07, Standard Test Method for Thermal Diffusivity by the Flash Method, ASTM International, West Conshohocken, PA, 2007.
- [7] ASTM E1269-11, Standard Test Method for Determining Specific Heat Capacity by Differential Scanning Calorimetry, ASTM International, West Conshohocken, PA, 2018.
- [8] S.E. Gustafsson, Transient plane source techniques for thermal conductivity and thermal diffusivity measurements of solid materials, Review of Scientific Instruments, 62 (1991) 797-804. [9] M. Gustavsson, E. Karawacki, S.E. Gustafsson, Thermal conductivity, thermal diffusivity, and
- specific heat of thin samples from transient measurements with hot disk sensors, Review of Scientific Instruments, 65 (1994) 3856-3859.
- [10] T. Log, S.E. Gustafsson, Transient plane source (TPS) technique for measuring thermal transport properties of building materials, Fire and Materials, 19 (1995) 43-49.
- [11] V. Bohac, M.K. Gustavsson, L. Kubicar, S.E. Gustafsson, Parameter estimations for measurements of thermal transport properties with the hot disk thermal constants analyzer, Review of Scientific Instruments, 71 (2000) 2452-2455.
- [12] H. Zhang, M.-J. Li, W.-Z. Fang, D. Dan, Z.-Y. Li, W.-Q. Tao, A numerical study on the theoretical accuracy of film thermal conductivity using transient plane source method, Applied Thermal Engineering, 72 (2014) 62-69.
- [13] M. Ahadi, M. Andisheh-Tadbir, M. Tam, M. Bahrami, An improved transient plane source method for measuring thermal conductivity of thin films: Deconvoluting thermal contact resistance, International Journal of Heat and Mass Transfer, 96 (2016) 371-380.
- [14] S.A. Al-Ajlan, Measurements of thermal properties of insulation materials by using transient plane source technique, Applied Thermal Engineering, 26 (2006) 2184-2191.
- [15] R.J. Warzoha, A.S. Fleischer, Determining the thermal conductivity of liquids using the transient hot disk method. Part I: Establishing transient thermal-fluid constraints, International Journal of Heat and Mass Transfer, 71 (2014) 779-789.
- [16] R.J. Warzoha, A.S. Fleischer, Determining the thermal conductivity of liquids using the transient hot disk method. Part II: Establishing an accurate and repeatable experimental methodology, International Journal of Heat and Mass Transfer, 71 (2014) 790-807.
- [17] S. Flueckiger, T. Voskuilen, Y. Zheng, T.e. Pourpoint, Advanced Transient Plane Source Method for the Measurement of Thermal Properties of High Pressure Metal Hydrides, in ASME

- 2009 Heat Transfer Summer Conference collocated with the InterPACK09 and 3rd Energy Sustainability Conferences, Vol. 1: Heat Transfer in Energy Systems; Thermophysical Properties; Heat Transfer Equipment; Heat Transfer in Electronic Equipment, 2009, pp. 215-221.
- [18] M. Gustavsson, S.E. Gustafsson, On the use of Transient Plane Source sensors for studying materials with direction dependent properties in: R. Dinwiddie, R. Mannello (eds.) 26th International Thermal Conductivity Conference/14th International Thermal Expansion Symposium, Vol. 26, Cambridge, MA, 2005, pp. 367-377.
- [19] ISO 22007-2:2015, Plastics Determination of thermal conductivity and thermal diffusivity Part 2: Transient plane heat source (hot disc) method, International Organization for Standardization, Switzerland, 2015.
- [20] Y. He, Rapid thermal conductivity measurement with a hot disk sensor: Part 1. Theoretical considerations, Thermochimica Acta, 436 (2005) 122-129.
- [21] M. Gustavsson, N.S. Saxena, E. Karawacki, S.E. Gustafsson, Specific heat measurements with the Hot Disk thermal constants analyser, in: K.E. Wilkes, R.B. Dinwiddie, R.S. Graves (eds.) Thermal conductivity 23, Interantional thermal conductivity conference, Nashville, TN, 1995, pp. 56-65.
- [22] A. Berge, B. Adl-Zarrabi, C.-E. Hagentoft, Determination of specific heat capacity by transient plane source, Frontiers of Architectural Research, 2 (2013) 476-482.
- [23] S. Farah, D.G. Anderson, R. Langer, Physical and mechanical properties of PLA, and their functions in widespread applications A comprehensive review, Advanced Drug Delivery Reviews, 107 (2016) 367-392.
- [24] Technical data sheet available at https://polymerdatabase.com/polymers/>.
- [25] M. Pyda, R.C. Bopp, B. Wunderlich, Heat capacity of poly(lactic acid), The Journal of Chemical Thermodynamics, 36 (2004) 731-742.
- [26] Technical data sheet available at https://omnexus.specialchem.com/polymer-properties/thermal-insulation#PS-X>.
- [27] A. Sarı, A. Biçer, C. Alkan, Poly(styrene-co-maleic anhydride)-graft-fatty acids as novel solid–solid PCMs for thermal energy storage, Polymer Engineering & Science, 59 (2019) E337-E347.
- [28] R. Guo, Z. Ren, H. Bi, M. Xu, L. Cai, Electrical and Thermal Conductivity of Polylactic Acid (PLA)-Based Biocomposites by Incorporation of Nano-Graphite Fabricated with Fused Deposition Modeling, Polymers, 11 (2019).